Brownian dynamics simulations in hydrogels using an adaptive time-stepping algorithm

Mats Kvarnström
Fraunhofer-Chalmers Research Centre, Chalmers Science Park, SE-412 88 Göteborg, Sweden
and Department of Applied Physics, Chalmers University of Technology, SE-412 96 Göteborg, Sweden

Aron Westergård and Niklas Lorén
SIK—The Swedish Institute for Food and Biotechnology, Box 5401, SE-402 29, Göteborg, Sweden

Magnus Nydén
Department of Chemical and Biological Engineering, Chalmers University of Technology, SE-412 96 Göteborg, Sweden
(Received 4 October 2007; published 8 January 2009)

The adaptive time-stepping algorithm for Brownian simulation of solute diffusion in three-dimensional complex geometries previously developed by the authors of this paper was applied to heterogeneous three-dimensional polymer hydrogel structures. The simulations were performed on reconstructed three-dimensional hydrogels. The obstruction effect from the gel strands on water and diffusion of dendrimers with different sizes were determined by simulations and compared with experimental nuclear magnetic resonance diffusometry data obtained from the same material. It was concluded that obstruction alone cannot explain the observed diffusion rates, but an interaction between the dendrimers and the gel strands should be included in the simulations. The effect of a sticky-wall interaction potential with geometrically distributed residence times on the diffusion rate has been studied. It was found that sticky-wall interaction is a possible explanation for the discrepancy between simulated and experimental diffusion data for dendrimers of different sizes diffusing in hydrogels.

DOI: 10.1103/PhysRevE.79.016102 PACS number(s): 82.20.Wt, 82.56.Lz, 68.05.Cf, 05.40.−a

I. INTRODUCTION

It is important to understand diffusion mechanisms of solutes in polymer-based hydrogels for the development of many industrial applications. In the pharmaceutical industry, for instance, the future most likely involves more sophisticated delivery systems. In order to decrease the time it takes for new drugs to reach the market it is very important from a drug delivery point of view to understand the intrinsic coupling between the physical properties of the solute or drug and the structure of the surrounding matrix in which the solute or drug is incorporated. Fundamental understanding of diffusion mechanisms in polymer gels is important also in other applications such as hygiene materials for instance. Here the swelling rate depends to a large extent on the flow and diffusion rates of small solutes into a polymer-based material. In future hygiene materials it may be foreseen that the material also will include other functions such as skin therapy and/or clinical testing, providing the possibility of early disease warning. Thus, a basic understanding of the processes governing solvent, solute, and polymer dynamics in these materials is of prime interest.

Previous works that combine microscopy and nuclear magnetic resonance (NMR) diffusometry have shown that there exists a strong correlation between the structure of the surrounding material matrix and the molecular diffusion properties in both hydrogels and emulsions [1,2]. There have been numerous attempts in the literature to theoretically model solute diffusion in hydrogels [3–5]. To our knowledge, however, a model has not yet been presented that successfully predicts diffusivity of small and large solutes in dilute and concentrated polymer gels. Some of the models presented work well for small solutes in crowded polymer solutions or gels and some work for small solutes in dilute polymer solutions or gels. There are many underlying problems with respect to obtaining a general model for predicting diffusivity in all types of systems. One of the largest problems is to deal with structural heterogeneity of porous materials.

In this paper a different approach is undertaken for improving the understanding of diffusion mechanisms in polymer gels. We argue that due to matrix heterogeneity it will be virtually impossible to find a theory that will predict mass transport based on material parameters for all combinations of materials and solutes. The approach undertaken is rather pragmatic at this stage and it is based on the use of Brownian motion simulations of solute diffusion in a three-dimensional polymer gel network structure [6,7]. In a previous paper [8], a statistical mathematical method was developed for reconstructing the three-dimensional structure of polymer gels based solely on two-dimensional transmission electron microscopy micrographs. This reconstructed three-dimensional structure is used here as the matrix for solute diffusion. The diffusion simulation used is a newly developed adaptive time-stepping algorithm presented in [9]. The effect of the dynamics of the polymer itself is here considered to be zero. Hence the local diffusion rate of a solute depends on the motion of the solute molecules themselves, on interactions between the polymer matrix and the solute, and also on the effective obstruction of the polymer material. In this paper the focus is on Brownian motion simulations of water and different-sized dendrimers in three-dimensional hydrogels, and we compare the resulting obstruction factors with experimental obstruction factors obtained using NMR diffusometry. Dendrimers are dendritic polymer molecules that are well suited for determination of the effects of structure and

interaction on the diffusion properties in polymer gels since the size and surface properties of dendrimers can be easily controlled. In addition, dendrimers are very monodisperse and they cannot reptate as common polymers.

II. NMR DIFFUSOMETRY

A. Theory

A common method to obtain diffusion constants, or distribution in diffusion constants, is the NMR diffusometry (NMRD) method. The method as such is relatively fast; it does not involve any labeling of molecules, atoms, or nuclei. It is noninvasive and rather simple to perform on modern NMR spectrometers since these most often are equipped with pulsed field gradient capabilities. NMRD has the advantage that the observation time may be easily changed to obtain the time-dependent diffusion constant and, in the best-case scenario, the long-time diffusion constant at long enough observation times. Today the method is limited to observation times between 0.01 and 10 s. When monitoring diffusion in crowded materials the experiment is usually carried out by the so-called stimulated echo technique. By this pulse sequence and for sine-shaped gradient pulses the normalized signal intensity echo decay for monodisperse and freely diffusing molecules follows the equation

$$I/I_0(g,\Delta,\delta,\tau,T) = \frac{1}{2}\exp\left(-\frac{T}{T_1}\right)\exp\left(-\frac{2\tau}{T_2}\right) \times \exp\left(-\gamma^2 g^2 \delta^2 \frac{(4\Delta-\delta)}{\pi^2} D\right), \quad (1)$$

where g is the gradient strength, Δ the observation time, δ the duration of the gradients, γ the gyromagnetic ratio, τ the separation between the two first radio-frequency pulses, and T the time separation between the second and third radio-frequency pulses. T_1 is the longitudinal relaxation time and T_2 the transverse relaxation time. When keeping the relaxation parameters constant and defining the k parameter as $k = \gamma^2 g^2 \delta^2 (4\Delta - \delta)/\pi^2$, Eq. (1) may be written as

$$I/I_0 = \exp(-kD).$$

Polymers are always polydisperse, and one common way to model this is to assume a distribution in diffusion coefficients, $P(D)$, and integrate over all diffusion constants according to

$$I/I_0 = \int_0^\infty P(D)\exp(-kD)dD. \quad (2)$$

A commonly used distribution for polymers is the log-normal density function:

$$P(D) = \frac{1}{D\sigma_{\log D}\sqrt{2\pi}}\exp\left(-\frac{(\log D - \log D_m)^2}{2\sigma_{\log D}^2}\right), \quad (3)$$

where D_m is the mass-weighted median self-diffusion coefficient and $\sigma_{\log D}$ is the standard deviation of the logarithm of the diffusion coefficient [10]. A mean diffusion coefficient can then be calculated from $\langle D\rangle = D_m \exp(\sigma_{\log D}^2/2)$ after fitting a combination of (2) and (3) to the data by using a Levenberg-Marquardt fitting routine.

Brownian dynamic simulations are capable of providing the NMR echo attenuation without relying on the short gradient pulse approximation [11]. For the pulse sequence commonly used for NMR diffusometry, the simulated phase shift ϕ caused by the diffusion of molecule i is given by

$$\phi_i = \gamma g\left(\int_{t_1}^{t_1+\delta} z_i(t)dt - \int_{t_1+\Delta}^{t_1+\Delta+\delta} z_i(t)dt\right) \simeq \gamma g\left(\sum_{j=a}^{a+b} z_{i,j} - \sum_{j=a+c}^{a+b+c} z_{i,j}\right)\Delta t,$$

where t_1 is the time of the application of the first gradient pulse. In the discretization procedure, the notation $z_j = z(t)$ with $j = a, b$, and c for $t = t_1, \delta$, and Δ is used [11]. The distribution of phase shifts $P(\phi)$ was obtained by simulating N spin trajectories using this adaptive time-stepping algorithm. Finally, the NMR echo attenuation was calculated from

$$E = \int_{-\infty}^{\infty} P(\phi)\cos(\phi)d\phi \simeq \frac{1}{N}\sum_{i=1}^{N}\cos\phi_i.$$

It is well known that the initial slope of the echo decay is directly related to the mean-square displacement [12]. Therefore, the apparent diffusion coefficient can be estimated from the initial slope of the echo decay. Alternatively, it is possible to estimate the apparent diffusion coefficient based on the mean-square displacement obtained from the starting position and the end position of each particle trajectory.

B. Experiments

The NMR diffusometry experiments were performed on a Varian Unity Inova 500 MHz spectrometer equipped with a diffusion probe supplied by DOTY Science. The probe provides 4.8 T/m at maximum current of 10 A. The stimulated echo pulse sequence was used in all experiments and the gradient pulse length was 4 ms. The maximum gradient strength was varied so at least a tenfold decrease in signal intensity was obtained.

III. RESULTS

The main goals with the adaptive time-stepping algorithm developed in [9] were to increase both the accuracy and speed of Brownian dynamics simulations, to be able to include the effect of simple particle-to-wall interactions, and to make the results useful for comparison with experimental NMR diffusometry results. This is done by adaptively increasing the time step and thereby the average spatial step taken far away from any structure that can perturb the diffusion trajectory. In contrast, if the diffusant on the other hand is situated close to a structure so that the structure may interfere with the trajectory with a certain probability, then the trajectory will be resolved more accurately. The idea is to put computational power where it is most needed.

In [9], the adaptive algorithm was validated in an open geometry in the form of spheres on a cubic lattice and for

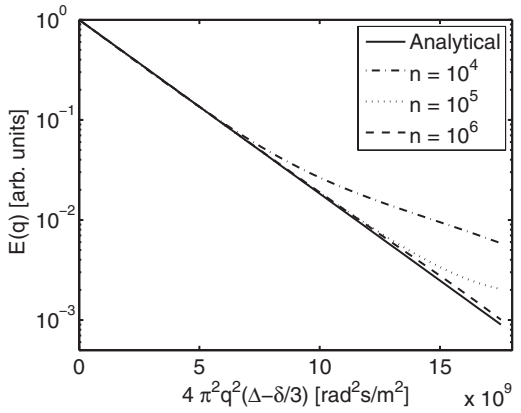

FIG. 1. Simulated NMR diffusometry echo decays $E(q)$ for free diffusion using the adaptive time-stepping algorithm developed in [9]. Results from simulations with different numbers of particles in comparison to the analytical solution (4) are shown. n is the number of particles used in the simulations. $\Delta=0.1$ s, $D=2\times10^{-9}$ m^2/s, $\delta=10^{-5}$ s, and $\gamma=26.751\times10^6$ rad/Ts.

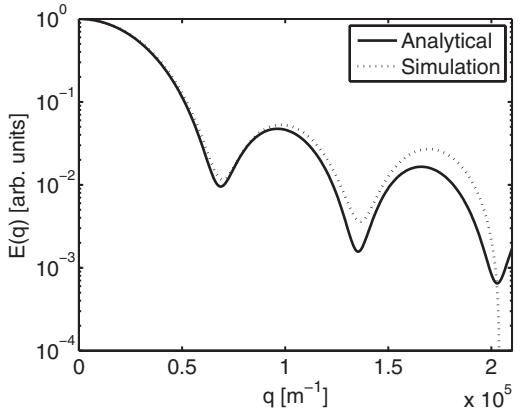

FIG. 2. Simulated NMR diffusometry echo decay for diffusion in a closed box using the adaptive time-stepping algorithm developed in [9]. The result of the simulation is compared with the analytical solution in (5). $\Delta=0.1$ s, $D=2\times10^{-9}$ m^2/s, $\delta=2$ ms, time step during gradients 2.5×10^{-9} s, voxel edge size 140 nm, box size 100^3 voxels, and 5×10^4 particles.

particles diffusing in a one-dimensional interaction potential [13]. Here, we will use the algorithm for comparison with NMR diffusometry data for systems with analytical solutions regarding the NMR signal and the diffusion equation. The large step is, however, to extend the methodology to real materials. Here, simulation results on diffusion of dendrimers with different sizes in three-dimensional polymer hydrogel structures will be presented and compared with experimental NMR diffusometry data.

A. Diffusion in systems with known analytical solution for NMR diffusometry

1. Free diffusion

The propagator $P(r_0|r,\Delta)$ is defined as the probability to find a molecule at a certain position r, after a certain observation time Δ, given that the molecule started at position r_0 at time zero. Note that the propagator is basically the van Hove function [14]. In a system with no boundaries and a Gaussian propagator, i.e., free diffusion, the echo decay using rectangular-shaped gradient pulses is described by [12]

$$E=\exp[-4\pi^2q^2D(\Delta-\delta/3)], \tag{4}$$

where $q=\gamma g\delta/2\pi$, Δ is the observation time, and D is the diffusion coefficient. The results for freely diffusing particles are shown in Fig. 1. The echo decays obtained from simulations are nearly identical to (4) as the number of particles exceeds 10^6. The relation between the estimated diffusion coefficient and the diffusion coefficient put into the simulations, D/D_0, is equal to 1.00 from evaluating both the initial slope of the echo decay and the actual mean-square displacement. D is the mean-squared displacement obtained using the adaptive time-stepping algorithm and D_0 is the analytical or exact diffusion coefficient. Figure 1 shows that approximately 10^5-10^6 particles are needed to obtain the fine details in the echo-decay at low intensities and high q values. However, if the main interest is to determine the diffusion coefficient, then approximately 10^4 particles are sufficient.

2. Diffusion in a confined geometry

Within the short gradient pulse limit and for arbitrary geometries, the echo decay can be written as [15]

$$E(\delta,\Delta,g)=\int\int\rho(r_0)P(r_0|r,\Delta)\exp[i\gamma g\delta(r-r_0)]dr\,dr_0,$$

where $\rho(r_0)$ is the spin density. To apply this relation to different geometries, knowledge about the specific propagator is required. The echo decay in a cube can be written as [11,12]

$$E(\delta,\Delta,g)=\frac{2[1-\cos(2\pi qL)]}{(2\pi qL)^2}+(4\pi qL)^2\times\sum_{n=1}^{\infty}\left[\frac{1-(-1)^n\cos(2\pi qL)}{[(n\pi)^2-(2\pi qL)^2]^2}\exp\left(-\frac{n^2\pi^2D\Delta}{L^2}\right)\right], \tag{5}$$

where L is the length between the walls of the cube. To attain the diffraction pattern described in the echo decay above it is necessary to use a diffusion time $\Delta>0.2L^2/D$. The results from the simulations in a closed box in comparison to the analytical solution are presented in Fig. 2. At low q values and intensities down to 10^{-2}, the analytical solution and the simulations match very well even if only 5×10^4 particles are used to simulate the echo decay. However, at high q values beyond the second minimum, the simulation starts to lack in precision. The reason for this is the limited number of particles used. The simulation for the free diffusion indicated that at least 10^5 particles are needed in order to further resolve the fine details in the echo decay.

B. Brownian simulations in three-dimensional gel structures

In previous work by Nisslert *et al.* [8], three-dimensional structures of sepharose gels have been identified by Markov chain Monte Carlo simulations based on image statistics

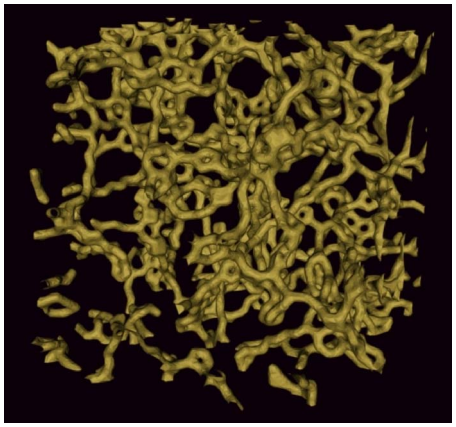

FIG. 3. (Color online) Identified three-dimensional sepharose gel structure. The side length of the cube is 800 nm.

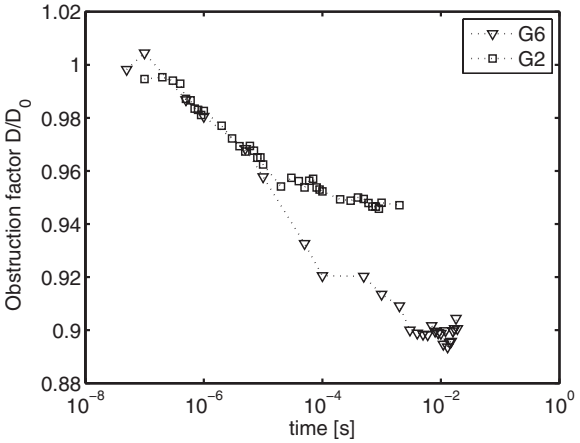

FIG. 4. Simulated obstruction factor D/D_0 as a function of observation time for dendrimers G_2 and G_6 in an identified 4% sepharose gel. The diffusion coefficients in pure water are $D_{G2}=5.61\times10^{-9}$ m^2/s and $D_{G6}=2.52\times10^{-9}$ m^2/s, respectively. The number of particles used in the adaptive simulation are $n_{G2}=4\times10^4$ and $n_{G6}=1.5\times10^4$.

from two-dimensional transmission electron microscopy micrographs. An example of an identified three-dimensional sepharose gel structure is shown in Fig. 3. The gel structure is very heterogeneous with large open regions and much more crowded and dense regions.

The objective of the performed Brownian motion simulations is to compare the gel strand obstruction effect on dendrimer and water obtained by the adaptive time-stepping algorithm with NMR diffusometry data on the same materials. Dendrimer diffusion in gels has been studied previously by [16] using NMR diffusometry. Here, two different dendrimer generations, G_2 and G_6, with different molecular weights and sizes were studied. Assuming a spherical shape, the radii of dendrimers G_2 and G_6 are approximately 3 and 8 nm, respectively.

1. Time-dependent obstruction in hydrogels

A lot of information about the structure in a certain material can be obtained by investigating the time dependence of the diffusion process. The time-dependent obstruction factor for dendrimers G_2 and G_6 diffusing in the same gel structures is shown in Fig. 4. The obstruction factor A is the ratio between the obstructed diffusion coefficient and the nonobstructed diffusion coefficient D/D_0. NMR diffusometry has been used to measure the diffusion coefficient in pure water and these values were used as D_0. At very short observation times, the dendrimers have not diffused far from their starting positions and few have encountered any gel strands. Therefore, the measured diffusion rate will coincide with the diffusion rate in pure water at very short observation times. However, at intermediate observation times the obstruction effect is more pronounced. This leads to a reduction of the effective diffusion rate.

The sizes of the dendrimer and water molecules are handled in the simulations by padding of the gel structure with the average radius of each type of molecule. Initially, the simulations of both dendrimers and water are performed by assuming no interactions between the surrounding gel matrix structure and diffusants, i.e., there will be a hard-core interaction between the diffusants and the gel matrix. At long enough observation times the global diffusion coefficient is obtained. The global diffusion coefficient is obtained at shorter observation times for dendrimer G_2 than for dendrimer G_6. The most obvious reason that dendrimer G_2 diffuses faster than dendrimer G_6 is its smaller size. Dendrimer G_2 thus samples all relevant gel structure more quickly than dendrimer G_6 and reaches the long-time limit more rapidly.

2. Obstruction in gels

Three different gel simulations were carried out. The first one simulated water diffusion. Water is small enough to be approximated by a single point; hence the original gel structure, here represented as R_0, was used. The two other gel structures are padded with 3 and 8 nm larger radius of the gel strands, R_3 and R_8, which correspond to the G_2 and G_6 dendrimers. Water, dendrimer G_2, and dendrimer G_6 were all simulated on three different identified gel structures. The results from the simulations and corresponding experimental NMR diffusometry results are displayed in Table I. The obstruction factor is defined as the ratio between the apparent diffusion coefficient obtained from simulations in gels and the diffusion coefficient in pure water. All simulated diffusion coefficients shown in Table I were calculated from both the initial slope of the NMRD echo decays and the mean-square displacement. No significant differences were found between these.

For water in the hydrogel the obstruction factors vary between 96.2% and 96.6% for simulations with 3×10^4 particles. This result coincides well with the NMR diffusometry result, which is $(96\pm1)\%$. It is very satisfying that the variation of the obtained obstruction factors for both water and dendrimers in the three different identified three-dimensional gel structures is small. This gives good confidence to both the identified gel structures and the adaptive time-stepping algorithm. For dendrimer G_2, with a padding of 3 nm, the resulting obstruction factors vary between 94.2% and 94.7%. However, NMR diffusometry gives an obstruction factor of $(82\pm1)\%$. Table I also shows that the simulated obstruction

TABLE I. Obstruction factors for diffusion in three different identified gel structures. R_0, R_3, and R_8 are different padding lengths believed to roughly correspond to water and the two dendrimers. The number of particles used in the simulations varied between 2×10^4 and 4×10^4. The simulation values were determined after 100 ms of simulations. The real dendrimers have ethylenediamine cores, polyamidoamine branches, and polyethyleneglycol surfaces. Dendrimers were supplied by Dendritic Nanotechnologies Inc. (DNT), Mount Pleasant, U.S.A. Two different generation were used, *G*2 (DNT-315) and *G*6 (DNT-319), having molecular weights of approximately 12 000 and 200 000 g/mol, respectively. Experimental data were taken from Jarvoll *et al.* [17].

	Gel 1 (%)	Gel 2 (%)	Gel 3 (%)	Expt. NMR-measurement (%)
R_0 (water)	96.6	96.3	96.2	(96 ± 1)
R_3 (*G*2 dendrimer)	94.7	94.2	94.5	(82 ± 1)
R_8 (*G*6 dendrimer)	90.1	89.8	89.8	(40 ± 1)

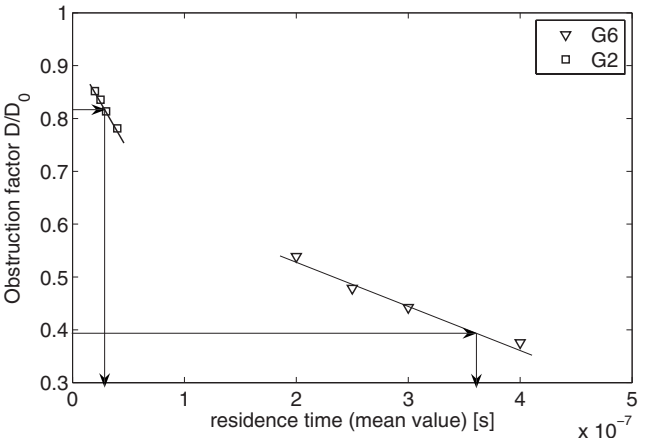

FIG. 5. Effect of different residence times on the obstruction factor. Sticky-wall interactions with geometrically distributed residence times are used in the adaptive simulations. The number of particles is 2×10^4 in all simulations.

factor for dendrimer G_6 varied between 89.8% and 90.1%. This should be compared with the obstruction factor of 40%, as reported by Jarvoll *et al.* [17]. The results clearly demonstrate that Brownian simulations give significantly higher diffusion coefficients than what is measured by NMR diffusometry for dendrimers G_2 and G_6. In contrast, the Brownian simulations work well for water diffusion. The results in Table I indicate that the reduction in diffusion rates for the dendrimers is due to both obstruction and interaction. It is, however, only the obstruction that is calculated by the present Brownian simulations. In a real material the reduction in diffusion rate may be affected by attractive or repulsive interactions between the diffusants and the gel matrix.

3. Sticky-wall interaction of dendrimers

One way to treat the interactions between dendrimers and gel matrix is to introduce a "sticky" boundary condition, meaning that the dendrimer basically becomes arrested for a very short moment in a small volume when it encounters the gel strand [18]. The stickiness can reflect dendrimer entanglement with the gel strand network or electrostatic interactions. One way to test a simple interaction between particles and walls through simulations is to implement a constant time delay every time a dendrimer reaches the gel strands. Applying such a delay time shows that 30 and 250 ns delay times are needed in the *G*2 and *G*6 simulations, respectively, in order to get good comparison between simulation and NMR diffusometry data. However, these delay times can just serve as indications of the interaction between dendrimers and gel strands. In order to simulate the interaction more physically correctly, escape probabilities based on interaction potentials should be included. This will result in a distribution of time delays.

Peters and Barenbrug [18] performed Brownian simulations with sticky-wall assumptions. They assumed that the stickiness of the wall can be described by a narrow but deep potential well, adjacent to a reflecting wall. If a particle resides in this well, it is defined as being stuck. In this work, we have used a geometric distribution to model the residence time on the gel strands. The reason for this is that using a probability that depends only on Δt (and not on how long the particle has resided at the wall) will generate a geometric distribution for the number of time steps a particle resides at a wall once it has stuck to it. This is coherent with the sticky-wall model in [18].

Figure 5 shows the obstruction factors for simulations with different mean values of the geometrical distribution. We have simulated four different mean values for dendrimers *G*2 and *G*6, respectively, using 2×10^4 particles and the same three-dimensional gel structure. It can be seen that the obstruction factor changes nearly linearly with the mean value of the geometrical distribution for both dendrimers *G*2 and *G*6 in the regimes studied in this work. Note that it is likely that the effect changes in a nonlinear fashion but that a linear approximation is used locally in Fig. 5 to simplify the estimation of the residence time. A comparison of the simulated results with experimental NMR diffusometry results presented in Table I shows that mean residence times of approximately 30 and 365 ns are required for dendrimers *G*2 and *G*6, respectively. This means that the effect of the residence time increases with the size of the dendrimer. Furthermore, the mean residence time for dendrimers *G*2 and *G*6 can be compared with the average distance that they would propagate during the residence time if they were free. Dendrimers *G*2 and *G*6 move in average about 1.5 and 7.4 nm during the average residence time, which should be compared with the radius of the dendrimers. Thus, if the sticky-wall condition reflects entanglement between the dendrimer and the gel strands, then the results indicate that dendrimer *G*6 has a more intricate interaction with the gel strands than dendrimer *G*2. This hypothesis is supported by the heterogeneous distribution of dendrimer end groups [19–21].

IV. DISCUSSION AND CONCLUSIONS

We have shown that an adaptive time-stepping algorithm performs well for different validation cases; free diffusion, diffusion in a box, and obstruction caused by sphere regu-

larly distributed in a cubic lattice. Using this technique we aim to estimate and predict the diffusion rate in the long-time limit in very complex three-dimensional structures such as supramolecular hydrogels. Three-dimensional hydrogel structures were obtained from transmission electron micrographs using a previously developed Markov chain Monte Carlo simulation technique. Particles were placed in these three-dimensional gels and our adaptive time-stepping algorithm was applied. The simulation results for water diffusion in three-dimensional gels showed good agreement with experimentally obtained diffusion rates using NMR diffusometry. This is not so surprising since the diffusion rate of small water molecules is expected to be mainly determined by obstruction, which is very small. However, the much larger dendrimers have much more complicated interactions with the surrounding structure than water. The simulation results from dendrimer diffusion in three-dimensional gels overestimate the dendrimer diffusion rate for both dendrimers *G*2 and *G*6 as compared with experimental NMR diffusometry data. The effects of the obstructions from the gel strand network and the finite size of the dendrimers were included in the simulations. This means that obstruction alone cannot explain the reduction of the dendrimer diffusion rate in supramolecular gels. Here, we have taken a very pragmatic approach by simply applying a sticky-wall boundary condition. The magnitude of the residence times found seems to be relevant and the simulation gives important indications of the processes controlling the diffusion rate. Furthermore, the spherical hard-sphere approximation of the dendrimer is a very coarse representation of the dendrimer. The dendrimer has a much more complex structure than that of a hard sphere [19–21]. Thus, the dendrimers interact with the gel strand network in a nontrivial way that retards the diffusion rate. However, more elaborate simulations based on physically relevant potentials will be needed in order to fully understand the interaction process between the dendrimers and the gel strands. It is, however, possible to explicitly simulate the trajectories of the particles under the influence of a particle-wall interaction potential. Initial simulations [9] strongly indicate that our adaptive time-stepping algorithm can be used for efficient future simulations in complex three-dimensional geometries when the particle-wall interaction is defined by an interaction potential.

ACKNOWLEDGMENTS

This work has been carried out with financial support from the Swedish Foundation for Strategic Research and the Swedish Research Council. M.K.'s work has been supported by the Swedish Foundation for Strategic Research through GMMC, the Gothenburg Mathematical Modelling Centre. The authors would like to express their gratitude toward Professor Mats Rudemo who has given valuable comments during the process of writing this paper.

[1] B. Walther, N. Lorén, M. Nydén, and A.-M. Hermansson, Langmuir **22**, 8221 (2006).
[2] N. Lorén, H. Hagslätt, M. Nydén, and A.-M. Hermansson, J. Chem. Phys. **122**, 024716 (2005).
[3] L. Masaro and X. Zhu, Prog. Polym. Sci. **24**, 731 (1999).
[4] B. Amsden, Macromolecules **32**, 874 (1999).
[5] J.-M. Petit, B. Roux, X. Zhu, and P. Macdonald, Macromolecules **29**, 6031 (1996).
[6] P. A. Netz and T. Dorfmüller, J. Chem. Phys. **103**, 9074 (1995).
[7] P. A. Netz and T. Dorfmüller, J. Chem. Phys. **107**, 9221 (1997).
[8] R. Nisslert, M. Kvarnström, N. Lorén, M. Nydén, and M. Rudemo, J. Microsc. **225**, 10 (2007).
[9] M. Kvarnström, A. Westergård, N. Lorén, and M. Nydén (unpublished).
[10] B. Håkansson, M. Nydén, and O. Söderman, Colloid Polym. Sci. **278**, 399 (2000).
[11] P. Linse and O. Söderman, J. Magn. Reson., Ser. A **116**, 77 (1995).
[12] W. Price, Concepts Magn. Reson. **9**, 299 (1997).
[13] T. Miyata, A. Endo, T. Ohmori, M. Nakaiwa, M. Kendo, K.-I. Kurumada, and M. Tanigaki, J. Chem. Eng. Jpn. **35**, 640 (2002).
[14] L. van Hove, Phys. Rev. **95**, 249 (1954).
[15] P. Callaghan, *Principles of Nuclear Magnetic Resonance Microscopy*, 1st ed. (Clarendon Press, Oxford, 1991).
[16] W. Baille, C. Malveau, X. Zhu, Y. Kim, and W. Ford, Macromolecules **36**, 839 (2003).
[17] P. Jarvoll, J.-E. Löfroth, H. Hagslätt, and M. Nydén (unpublished).
[18] E. A. J. F. Peters and T. M. A. O. M. Barenbrug, Phys. Rev. E **66**, 056702 (2002).
[19] B. Klajnert and M. Bryszewska, Acta Biochim. Pol. **48**, 199 (2001).
[20] M. Mansfield and L. Klushin, Macromolecules **26**, 4262 (1993).
[21] S. V. Lyulin, A. A. Darinski, A. V. Lyulin, and M. Michels, Macromolecules **37**, 4676 (2004).